http://app.pan.pl/SOM/app55-Ciurej_SOM.pdf

SUPPLEMENTARY ONLINE MATERIAL FOR

Procedures for obtaining optimal SEM images of coccolithophore debris in coccolith limestones

Agnieszka Ciurej

Published in *Acta Palaeontologica Polonica* 2010 55(1): 169-171.

This supplement contains: Supplementary **Text and Figures S1 – S7**

Fig. S1 shows an image of coccolith debris obtained in ESEM under low vacuum from non-coated polished thin section using charge contrast imaging (CCI).

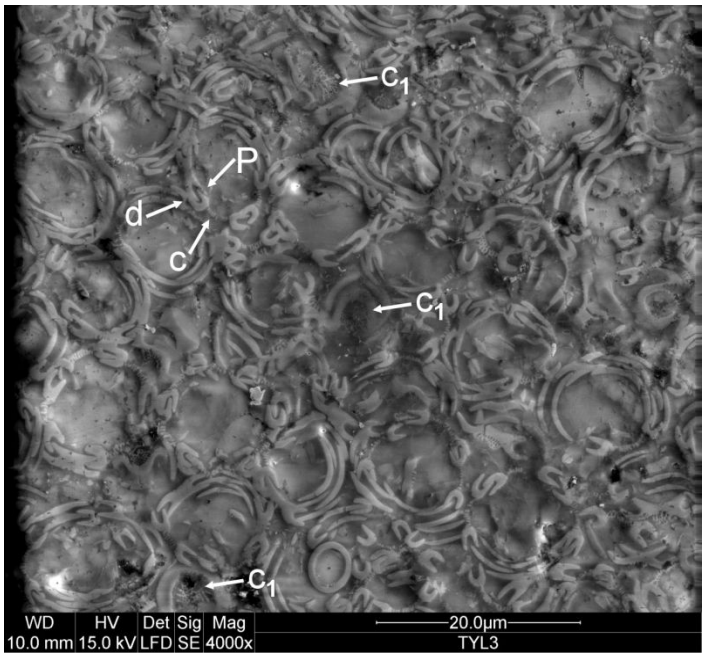

Fig. S1. CCI image of coccolith debris in the central part of a fossil faecal pellet from microlaminated coccolith limestone. Cross-sections of complete and dismembered, variously oriented coccospheres allow us to observe their structure. Perpendicular cross-sections of coccospheres allow to observe distal (d) and proximal (p) shields of placoliths, joined by parallel calcite crystallites in the wide central area (c), situated on a proximal part of the placoliths. The interlocking of adjacent edges of placolith shields is also well visible. Structures closing the central area (c_1) are seen as a net in horizontal view on variously orientated sections of plates. Note the same characteristics of tightly packed coccospheres over the whole image. Well discernible are also such diagenetic features as cement within and around coccospheres as well as separate coccolith plates in various stages of diagenesis. The image was obtained from a well polished non-coated thin section in SE image in ESEM using WD - 10.0 mm and SS - 37s/frame, ZNG PAN B-III-75/1.

Coccolith material may become hardly recognisable in BSE images obtained from non-coated thin sections in low vacuum. Both the coccolith material and the cement have the same chemical composition, hence they appear alike in the images (Fig. S2). Outlines of hollow coccospheres are discernible in the BSE images when they are filled with material that is different in chemical composition than the coccoliths (Fig. S3). Coccolith material may be also recognisable in the BSE images because of the higher porosity of the less cemented limestone around them (Fig. S4).

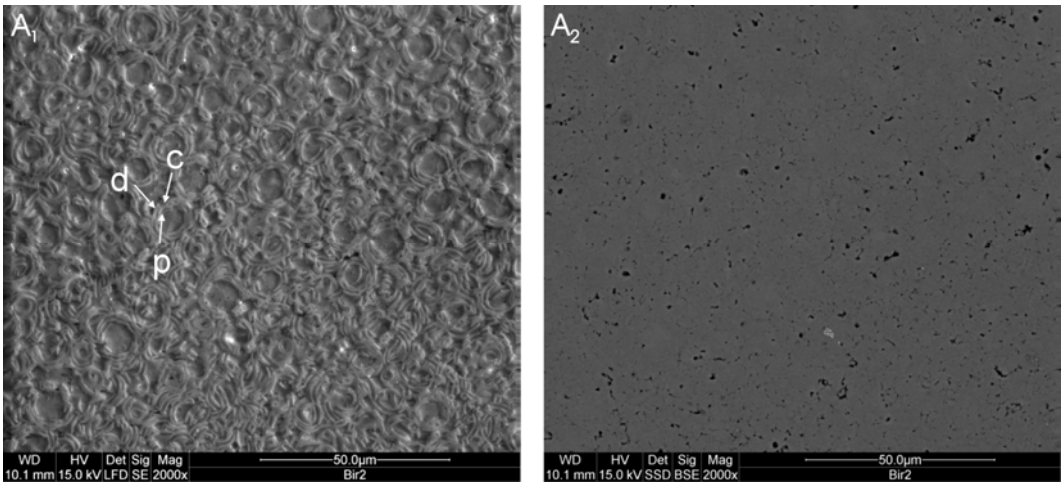

Fig. S2. Comparison of CCI (A_1) and BSE (A_2) images of coccospheres tightly packed in a faecal pellet, obtained in ESEM under low vacuum from non-coated polished thin section: A_1 - SE, WD - 10.1 mm, SS - 37 and A_2 - BSE, WD - 10.1 mm, SS - 32 s/frame. Distal (d) and proximal (p) shields of placoliths and central area (c) are well visible in A_1. Note the same characteristics of these structures seen in Fig. 1B (main text). The coccolith material becomes indistinguishable from cement in BSE image (A_2), because of the same chemical composition. Porosity (black) is well visible instead, ZNG PAN B-III-75/4.

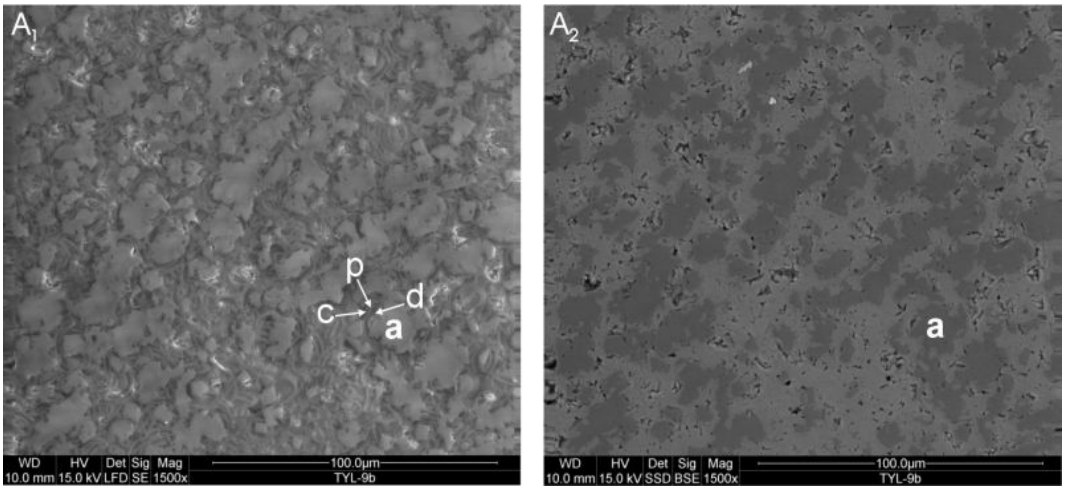

Fig. S3. Comparison of CCI (A_1) and BSE (A_2) images of complete and dismembered coccospheres packed in a faecal pellet and filled with silica of diagenetic origin. ESEM under low vacuum of non-coated polished thin section: A_1 - SE, WD - 10.0 mm, SS - 37 s/frame and A_2 - BSE, WD - 10.0 mm, SS - 32 s/frame. In CCI, details of the coccoliths are well discernible in some coccospheres only (a). Note distal (d) and proximal (p) shields of placoliths and central area (c). In BSE image (A_2) the coccolith material, especially coccospheres, can be traced as outlines only (a), ZNG PAN B-III-75/2.

The differences related to chemical composition are well visible in BSE in both the coated and non-coated samples (Figs. S2 – S6). In the BSE images, the mineral grains with relatively high average atomic numbers and higher backscatter coefficients (e.g., pyrite and quartz) produce brighter images in comparison to organic matter and carbon-based resins. These have low average atomic numbers (and thus low backscatter coefficients) and produce darker images (see Pike and Kemp 1996).

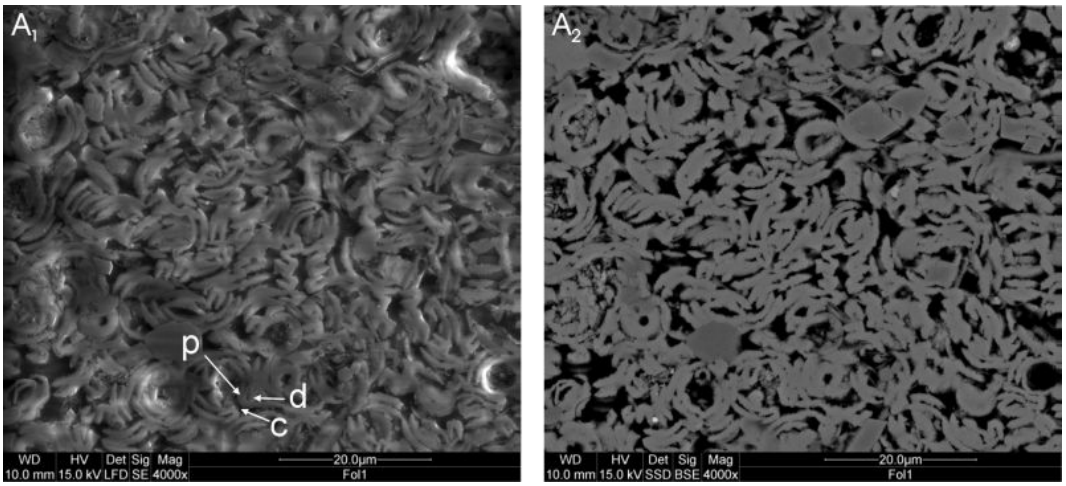

Fig. S4. Comparison of CCI (A_1) and BSE (A_2) images of complete and dismembered coccospheres obtained in ESEM under low vacuum from non-coated polished thin section: A_1 - SE, WD - 10.0 mm, SS - 37 s/frame and A_2 - BSE, WD - 10.0 mm, SS - 32 s/frame. Structural details such as distal (d) and proximal (p) shields of placoliths and central area (c) are well visible in CCI. Outlines of coccoliths are discernible in BSE, only owing to the high porosity (black colour), ZNG PAN B-III-75/5.

Coccolith debris becomes unrecognisable in SE in low vacuum when the samples are coated even with the thinnest carbon film (Fig. S5). The adverse effect of the carbon coating is similar in both the SE and BSE images in high vacuum (Fig. S6). Coccolith debris may be discernible in coated samples in high vacuum in BSE when they are surrounded by material with contrasting chemical composition or porous. The quality of coccolith details is similar as in BSE images obtained under low vacuum.

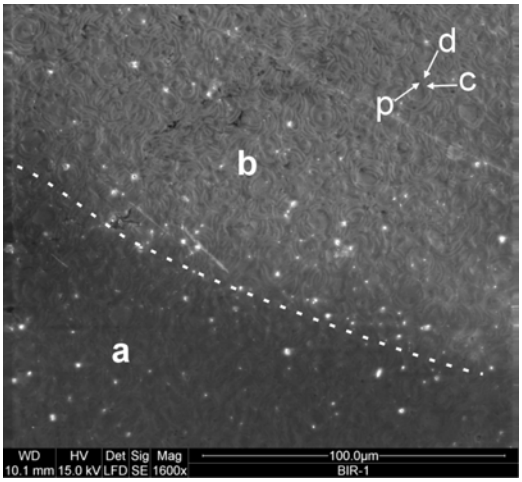

Fig. S5. A test image of a specimen carbon-coated in its lower left part (a) and non-coated in the upper part, behind the dotted line (b), obtained in ESEM in low vacuum, SE mode. WD - 10.1 mm, SS - 37 s/frame. Coccolith material with structural details, such distal (d) and proximal (p) shields of placoliths and central area (c) is well discernible in the non-coated part (b), and becomes gradually obliterated under the thickening coating (a), ZNG PAN B-III-75/4.

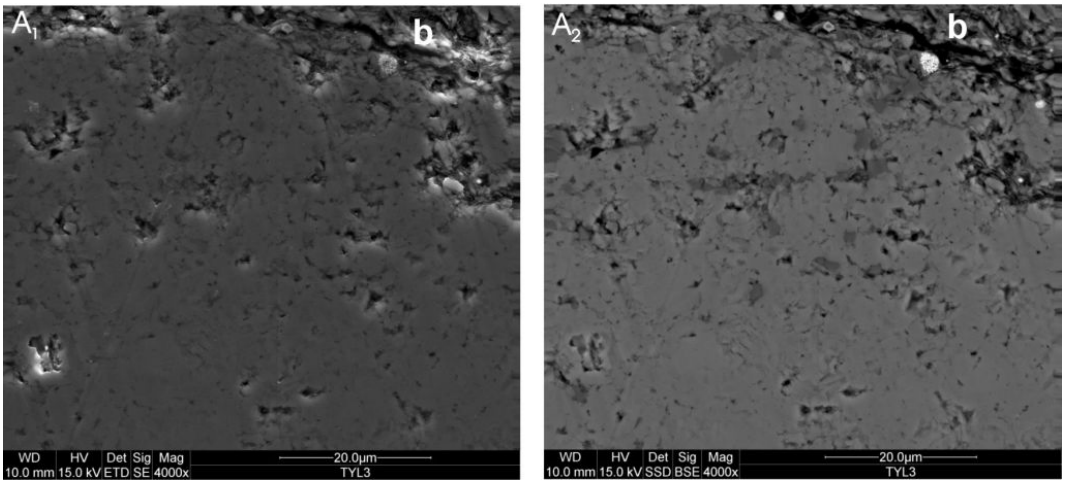

Fig. S6. Images of the upper marginal part of the faecal pellet seen in Fig. S1 obtained after coating with carbon. ESEM under high vacuum: A_1 - SE - WD - 10.0 mm, SS - 37 s/frame and A_2 - BSE - WD - 10.0 mm, SS - 32 s/frame. The coccolith material, seen in Fig. S1, is unrecognisable. Differences in chemical composition are shown as shades of brightness in BSE image (A_2). Note the pyrite grains (bright) near the pellet boundary (b), ZNG PAN B-III-75/1.

Studying the same polished thin sections under optical microscope and ESEM enables the precise location of the studied details within the sequence of microlaminae and their internal elements, in laminated limestones (Fig. S7).

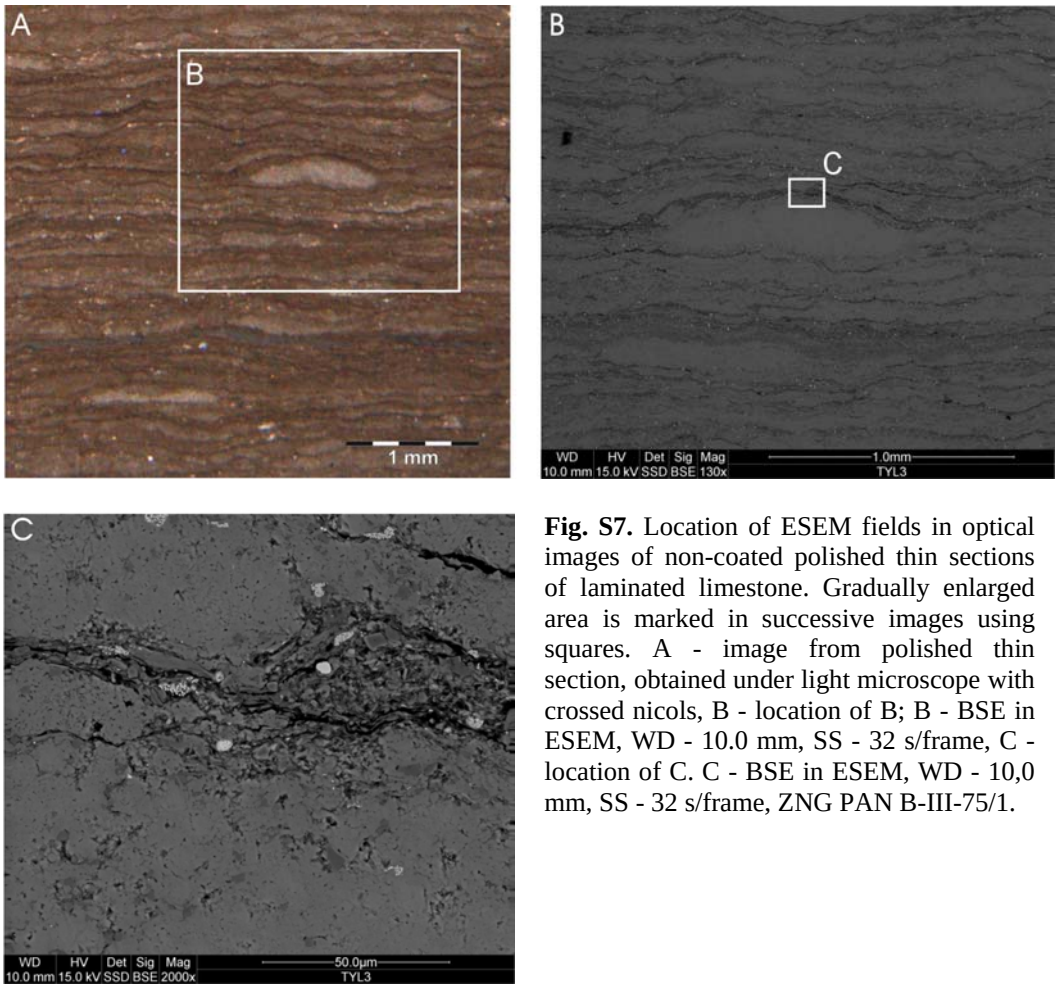

Fig. S7. Location of ESEM fields in optical images of non-coated polished thin sections of laminated limestone. Gradually enlarged area is marked in successive images using squares. A - image from polished thin section, obtained under light microscope with crossed nicols, B - location of B; B - BSE in ESEM, WD - 10.0 mm, SS - 32 s/frame, C - location of C. C - BSE in ESEM, WD - 10,0 mm, SS - 32 s/frame, ZNG PAN B-III-75/1.

References

Pike, J. and Kemp, A.E.S. 1996. Preparation and analysis techniques for studies of laminated sediments. In: Kemp, A.E.S. (Ed.), Palaeoclimatology and Palaeoceanography from Laminated Sediments. *Geological Society London Special Publication* 116: 37-48.